

The influences of outflow on the dynamics of inflow

Fu-Guo Xie,^{1,2,3} Feng Yuan^{1,2}

ABSTRACT

Both numerical simulations and observations indicate that in an advection-dominated accretion flow most of the accretion material supplied at the outer boundary will not reach the inner boundary. Rather, they are lost via outflow. Previously, the influence of outflow on the dynamics of inflow is taken into account only by adopting a radius-dependent mass accretion rate $\dot{M} = \dot{M}_0(r/r_{\text{out}})^s$ with $s > 0$. In this paper, based on a 1.5 dimensional description to the accretion flow, we investigate this problem in more detail by considering the interchange of mass, radial and azimuthal momentum, and the energy between the outflow and inflow. The physical quantities of the outflow is parameterized based on our current understandings to the properties of outflow mainly from numerical simulations of accretion flows. Our results indicate that under reasonable assumptions to the properties of outflow, the main influence of outflow has been properly included by adopting $\dot{M} = \dot{M}_0(r/r_{\text{out}})^s$.

Subject headings: accretion, accretion disks — black hole physics — hydrodynamics — ISM: jets and outflows

1. Introduction

There are now strong observational evidences for the existence of outflow in accretion flow system. One of the best examples comes from Sgr A*, the supermassive black hole located at our Galactic center. The accretion flow in this source is likely in the form of the advection-dominated accretion flow (ADAF, or radiatively inefficient accretion flow; Yuan, Quataert & Narayan 2003). On one hand, from the observational results from *Chandra* combined with the Bondi accretion theory we can calculate the value of the mass accretion

¹Shanghai Astronomical Observatory, 80 Nandan Road, Shanghai 200030, China

²Joint Institute for Galaxy and Cosmology (JOINGC) of SHAO and USTC

³Graduate School of the Chinese Academy of Sciences, Beijing 100039, China; fgxie@shao.ac.cn

rate at the outer boundary—the Bondi radius. On the other hand, radio polarization observations constrain the accretion rate at the innermost region of the accretion flow nearly two orders of magnitude lower than that determined at the Bondi radius (e.g., Marrone et al. 2006). This implies that about 99% of the material available at the Bondi radius will not finally enter into the black hole horizon, rather, they must be lost in the form of outflow. Outflow seems to exist also in more luminous sources whose accretion mode is different from the ADAF. For example, the blueshifted absorption lines, which indicates the existence of outflowing materials, have been detected in the X-ray spectrum of some Seyfert 1 sources (e.g., NGC 3783: Kaspi et al. 2001) and more spectacularly in quasars (e.g., PG 1115+80: Chartas, Brandt & Gallagher 2003). The existence of outflow has been paid more and more attention recently in the field of galaxy formation because of its feedback effect in the co-evolution of galaxy and the central active galactic nuclei (e.g., Silk & Rees 1998; Granato et al. 2004; Springel et al. 2005).

Many work has been done on the origin and dynamics of outflow (e.g., Xu & Chen 1997; Blandford & Begelman 2004; Xue & Wang 2005) in the frame of self-similar hydrodynamical solution. Magnetic field, especially its poloidal component, may presumably serve as the most promising mechanism on producing outflow, as proposed by, e.g., Blandford & Payne (1982). This has been confirmed in non-radiative magnetohydrodynamical (MHD) numerical simulations of accretion flows (e.g., Stone & Pringle 2001; Igumenshchev et al. 2003; Vlahakis & Königl 2003; McKinney 2006). Radiation pressure could be another important mechanism in luminous accretion disk (Proga 2003). But even in the absence of magnetic field and strong radiation, outflow is likely present in ADAFs. This is first proposed from analytical argument that the Bernoulli parameter of an ADAF is large or even positive because of the small radiative energy loss. This implies that the gas is inclined to escape once they are perturbed (Narayan & Yi 1994; Blandford & Begelman 1999). This suggestion was later confirmed by numerical simulation by Stone, Pringle & Begelman (1999).

Since the outflow is likely very strong (Misra & Taam 2001), they may provide an additional important sink of angular momentum and energy. So it is important to investigate its dynamical influence to inflow. This problem has been investigated by Kuncic & Bicknell (2007) in the context of the standard thin disk. In this paper we focus on ADAFs. Blandford & Begelman (1999, hereafter BB99) examined this question through a one-dimensional self-similar approach. A phenomenological way was adopted in which they parameterized the rate at which mass, angular momentum and energy are extracted through outflow, regardless the mechanism of the formation of outflow.

BB99 gives a quite general description, covering a broad kind of outflow including Poynting flux whose mass flux is zero while energy flux is not. It is based on self-similar assumption.

For the purpose of application and comparison with observation, however, we need to discuss it based on global solutions, because self-similar solution is too simplified to be used to calculate the emitted spectrum. Quataert & Narayan (1999) presented the first effort on this aspect. They calculate the global solution of inflow when strong outflow is present by using a radius-dependent mass accretion rate, $\dot{M} \propto r^s$ while keeping all other equations describing inflow such as the momentum and energy equations unchanged. This is roughly equivalent to assuming that the specific angular momentum and energy of outflow is identical to the inflow at the same radius where outflow is launched (see e.g., eqs.(1)-(5)). This approach is subsequently adopted in almost all following works (e.g., Yuan, Quataert & Narayan 2003). In this paper, we refer to this treatment as standard treatment.

While the approximation of Quataert & Narayan (1999; see also Yuan, Quataert & Narayan 2003) may capture the most important influence of outflow to inflow, it is not obvious in what degree we can use this approximation or how good this approximation is when we compare the theoretical prediction such as the spectrum to observations. This is the aim of the present paper. More specifically, by considering the conservations of fluxes of mass, momentum, and energy of the combined inflow/outflow system, we focus on the influence of outflow on the dynamics of inflow. We will use a “1.5 dimension” description of the accretion flow, which means the height-integrated equations will be used instead of a fully two-dimensional description, but the conservation equations take into account the outflow in the vertical direction as well. The paper is organized as follows: in §2 we present basic equations for our model and discuss the main properties of outflow. The calculation results are presented in §3. The last section is devoted to a summary.

2. Accretion Model with Outflow

2.1. Basic Equations

We adopt a cylinder coordinate (r, ϕ, z) to describe a steady axisymmetric ($\partial/\partial t = \partial/\partial\phi = 0$) accretion flow. The Paczyński & Wiita potential (Paczynski & Wiita 1980) $\psi = -GM_{BH}/(r - r_g)$ is adopted to mimic the geometry of a Schwarzschild black hole, with M_{BH} is the mass of black hole and $r_g \equiv 2GM_{BH}/c^2$ is the Schwarzschild radius of the black hole. As shown in Fig. 1, we divide the whole accretion flow at each radius into two parts, i.e., inflow and outflow. For the inflow, we assume a hydrostatic balance in vertical direction ($v_z = 0$ for the inflow) and assume all quantities such as the radial and azimuthal velocity (v_r and v_ϕ), ions and electron temperature (T_i, T_e) and the sound speed (c_s) are only functions of radius r . Such an isothermal assumption in the vertical direction results in a density distribution of $\rho(r, z) = \rho(r, 0) \exp(-z^2/2H^2)$ in the inflow, where $H = c_s/\Omega_K$ is the vertical

scale height of inflow¹. We set $z = H$ as the surface where an outflow launches. The vertical gradients of above quantities are absorbed by their discontinuity between inflow and outflow at this surface, except that the density distribution is continuous and the density of outflow at $z = H$ is then $e^{-1/2}\rho(r, 0)$. Note that the vertical velocity of outflow $v_{z,w}$, will “compress” the inflow because of momentum conservation, thus the vertical scale height may be smaller. We neglect this effect here.

From compressible Navier-Stokes equations, we can write the equations of the conservations of mass, momentum, and energy for the inflow as follows (see Appendix A for details):

$$\frac{d\dot{M}(r)}{dr} = \eta_1 4\pi r \rho v_{z,w} \quad (1)$$

$$v_r \frac{dv_r}{dr} + \eta_1 v_{z,w} \frac{v_{r,w} - v_r}{H} = r(\Omega^2 - \Omega_k^2) - \frac{1}{\rho} \frac{dP}{dr} - \frac{1}{2} \frac{dc_s^2}{dr} \quad (2)$$

$$\rho r v_r \frac{d}{dr}(r^2 \Omega) + \eta_1 r^2 \rho v_{z,w} \frac{v_{\phi,w} - v_\phi}{H} = \frac{1}{H} \frac{d}{dr}(r^2 H \tau_{\phi r}) \quad (3)$$

$$\rho v_r \left(\frac{d\epsilon_e}{dr} - \frac{p_e}{\rho^2} \frac{d\rho}{dr} \right) + \eta_1 \rho v_{z,w} \frac{\epsilon_{e,w} - \epsilon_e}{H} = \delta q^+ + q_{ie} - q^- \quad (4)$$

$$\rho v_r \left(\frac{d\epsilon_i}{dr} - \frac{p_i}{\rho^2} \frac{d\rho}{dr} \right) + \eta_1 \rho v_{z,w} \frac{\epsilon_{i,w} - \epsilon_i}{H} = (1 - \delta) q^+ - q_{ie} \quad (5)$$

Here all quantities have their usual meanings. The specific internal energy of electrons and ions are ϵ_e, ϵ_i , respectively. The pressure P is the sum of gas and magnetic pressure $P = P_{gas} + P_{mag}$. The inflow’s accretion rate is defined as $\dot{M}(r) \equiv -4\pi r \rho v_r H$ and $\eta_1 \equiv \rho_w / \bar{\rho}$ is the density ratio of outflow and inflow (Appendix A). Parameter δ describes the fraction of the turbulent energy dissipation rate q^+ ($\equiv \tau_{\phi r} r d\Omega/dr$) that heats electrons directly. Energy transfers from ions to electrons through Coulomb collisions at a volume rate q_{ie} , and radiative cooling rate is denoted by q^- . The quantities with subscript w denote the quantities of wind/outflow just away from the launching surface $z = H$. We take the α viscosity description for the stress tensor $\tau_{\phi r}$ (Shakura & Sunyaev 1973):

$$\tau_{\phi r} = -\alpha P \quad (6)$$

where α is the dimensionless viscosity parameter. Other stress tensor components are neglected for simplicity, except that the ϕz component is considered by taking into account the angular momentum exchange between inflow and outflow at $z = H$.

¹This kind of vertical density structure is based on a first-order expand of Paczyński & Wiita potential, which is not exact far away from the equatorial plane (Gu & Lu 2007).

Obviously, it is impossible to directly solve the eqs. (1)-(5). We therefore introduce the following parameters “ ξ ” to evaluate the radial, azimuthal, and vertical velocity, and the ion and electron temperatures of outflow in terms of inflow,

$$v_{r,w} = \xi_r v_{ff}, \quad (7)$$

$$v_{\phi,w} = \xi_\phi v_\phi, \quad (8)$$

$$v_{z,w} = \xi_z c_s, \quad (9)$$

$$T_{i,w} = \xi_{T_i} T_i, \quad (10)$$

$$T_{e,w} = \xi_{T_e} T_e. \quad (11)$$

Here v_{ff} are the free-fall velocity, v_ϕ , and c_s are azimuthal velocity and the sound speed of the inflow, respectively. We assume that these parameters are independent of radius. While this assumption is simple, we think it can capture the main physics of the influence of outflow in a reasonable way. Specifically, this simple assumption does not mean all quantities are a power-law function of radius as the usual “power-law” assumption of the mass flux of inflow. If we know the values of these parameters, we will be able to get the global solution of eqs. (1)-(5).

2.2. Outflow’s Properties

We now estimate the properties of outflow. Generally all these quantities should be a function of z . Here we consider the properties of outflow when they are just launched or detached from inflow. All their subsequent evolution should be due to outflow itself and does not affect the inflow any longer.

The first quantity is the strength of the outflow, or the mass lost rate. BB99 assume $\dot{M} \propto r^s$ with $0 \leq s < 1$. This ensures that the mass accretion rate decreases while the released energy increases with accretion (BB99). The strength of outflow in our notion is mainly governed by ξ_z . The above range corresponds to $0 \leq \xi_z < -v_r/\eta_1 c_s \approx 0.2$ (ref. eq. (12), but note $s(r)$ now is a function of r).

We next consider the value of ξ_ϕ . The vertical distribution of angular momentum of the accretion flow is complicated. Two-dimensional self-similar analysis on ADAF based on hydrodynamics shows that the specific angular momentum of outflow is lower than inflow (Narayan & Yi 1995; Xu & Chen 1997; Blandford & Begelman 2004). This result is confirmed later by numerical simulations (e.g., Stone, Pringle & Begelman 1999). However, any magnetic coupling between inflow and outflow will likely lead to transportation of angular

momentum from the former to latter (Spruit 1996; Stone & Pringle 2001; BB99; Blandford & Begelman 2004). Therefore in this paper we explore ξ_ϕ in a range around unity, $0.8 < \xi_\phi < 1.2$.

Hydrodynamical and MHD simulations also reveal that the specific internal energy or the temperature of the gas increases from the equator to higher altitude (e.g., Stone, Pringle & Begelman 1999; De Villiers et al. 2005; Beckwith, Hawley & Krolik 2008). One underlying reason may be that the gas with higher internal energy may escape more easily. We therefore consider $\xi_{T_i} = 1, 1.5$ and $\xi_{T_e} = 1, 1.5$.

It is highly unclear about the radial velocity of outflow when they are just launched although we somehow know how they will be accelerated later. But we speculate that it should be positive, and should not be larger than a fraction of the local Keplerian or free-fall velocity v_{ff} . Fortunately, although it may be important for the dynamics of outflow itself, we find that the value of ξ_r has minor effect on the inflow. We simply set $\xi_r \equiv 0.2$ in our calculations.

3. Results

For our specific model, we adopt the black hole mass $M_{BH} \equiv 4.0 \times 10^6 M_\odot$, accretion rate at the outer boundary $r_{out} = 10^4 r_s$ is $\dot{M} = 1.1 \times 10^{-5} \dot{M}_{Edd}$, where $\dot{M}_{Edd} = 10 L_{Edd}/c^2$, is the Eddington accretion rate. The values for other parameters are $\alpha = 0.1, \beta \equiv P_{gas}/P_{total} = 0.9, \delta = 0.3$. These parameters are close to those in Yuan, Quataert & Narayan (2003) to model the supermassive black hole in our Galactic center. There they assume $\dot{M} \propto r^s$ with $s = 0.27$ being a constant. Under our notation, we have

$$s(r) = \frac{d \ln \dot{M}(r)}{d \ln r} = \eta_1 \xi_z \frac{v_k}{-v_r}, \quad (12)$$

where v_k is the Keplerian velocity. We would like to note that $s(r)$ now is not a constant as in Yuan, Quataert & Narayan (2003) (or Quataert & Narayan 1999). The slope of $\dot{M}(r)$ now is steeper at large radius while flatter at small radius, because of the quicker increase of v_r compared to v_k . This is shown in Fig. 2, where we adjust the parameter ξ_z so that the accretion rates at r_{out} and horizon are the same as the case of $\dot{M} \propto r^s$ with $s = 0.48$.

We first investigate the effect of ξ_z . Fig. 3 shows the effects of various ξ_z on inflow, with other outflow parameters fixed at $\xi_\phi = \xi_{T_e} = \xi_{T_i} = 1.0$ and $v_{r,w} = v_r$. The four plots show the Mach number, profiles of density, temperature, and specific angular momentum. The dotted, dashed, and long-dashed lines correspond to $\xi_z = 0.01, 0.05$ and 0.15 , respectively. As the outflow becomes stronger (ξ_z increases), the gas density decreases while the ion temperature

decreases. This is very similar to the case of the standard treatment (with increasing s). The decrease of ions temperature is because when more and more accretion material is lost via the outflow, the density profile becomes flatter thus the compression work which is an important heating mechanism for ions becomes weaker. Different from the ions, the electrons temperature has no obvious relation with the strength of outflow. This is because different from ions the compression work in the electron energy equation is about one order of magnitude smaller due to the lower electron temperature (ref. eq. 4).

We mentioned before that the value of the radial velocity of outflow or equivalently ξ_r , has minor effect on the dynamics of inflow. The “kick back” force due to the discrepancy of the radial velocity between the inflow and outflow is manifested by the second term in eq. (2). Since $v_{z,w} = \xi_z c_s$, $H = c_s/\Omega_k$ and $v_r \sim \alpha v_k$, this term is roughly $\alpha \xi_z (\ll 1)$ times of the gravitational force thus can be neglected. So we simply fix $\xi_r = 0.2$ in this paper.

We now check how good the standard treatment is. For this purpose, we first get the global solution with the standard treatment with $\dot{M} = 2 \times 10^{-5} (r/r_{out})^{0.25}$ and $r_{out} = 10^4 r_g$. We then get the global solution of eqs. (1) - (5) for various sets of outflow parameters of $\xi_\phi = 0.8, 1.0, 1.2$, $\xi_{T_i} = 1.0$ (referred to Case A) and 1.5 (referred to as Case B), and $\xi_{T_e} = 1.5$. For each set of these parameters, we adjust the value of ξ_z so that the mass accretion rates at r_{out} and black hole horizon are equal to the values in the above standard treatment. By doing this, we want to focus on the influence on inflow of the transportation of angular momentum and internal energy between inflow and outflow, which is neglected in the standard treatment. Note the profile of accretion rate in this case is similar to Fig. 2.

Fig. 4 shows the comparison of Case A with the standard treatment. We can see that our models intend to have lower densities compared to the standard treatment, although the accretion rates at the outer and inner boundaries are the same. We can easily understand this by looking at bottom-left panel of Fig. 4. Our solutions have higher ion temperature and lower electron temperature at the inner region of the inflow. The higher ion temperature is because the density profile in the inner region is steeper thus the compression heating is stronger. The lower electron temperature is because $\xi_{T_e} = 1.5 > 1$ which implies that some internal energy is transferred into the outflow from inflow (ref. eq. 4).

Fig. 5 shows the dynamical influences of outflow for Case B. Compared to Case A, the ion temperature is lower. This is obviously because ξ_{T_i} is larger, $\xi_{T_i} = 1.5$, so some internal energy is transferred from inflow to outflow. The lower ion temperature results in a smaller H . This, combined with the smaller radial velocity, make the density of inflow higher compared to Case A and almost identical to that of the standard treatment, as shown in the figure. We also see from the figure that both the value of the specific angular momentum and its slope are higher compared to the standard treatment. This results in a stronger

viscous heating, which somehow cancel the effect of $\xi_{T_e} = 1.5 > 1$. This is why the electron temperature is roughly the same with the standard treatment while higher than that of Case A.

From Fig. 3 to 5, we find that within the range of the values of parameters we adopt to describe the outflow, the strength of the outflow has the most significant influence on the dynamics of inflow (i.e., Fig. 3). The influences of all other properties of outflow, namely the angular momentum, temperature, and radial velocity, are much smaller (Figs. 4 and 5). This is the reason why the discrepancy between our model (with different properties of outflow) and the standard treatment, which only considers the strength of outflow but assume the properties of outflow are the same with inflow, is small.

4. Summary

Outflow is now believed to be very significant in advection-dominated accretion flow thus it is important to investigate their influence on the dynamics of inflow. Previously this was done by using a rather simple way. In the “standard treatment” the only change compared to the case of no outflow is that the mass accretion rate is not a constant, but a power-law function of radius, $\dot{M} \propto r^s$ ($s > 0$). All other equations describing the accretion flow remain unchanged (e.g., Quataert & Narayan 1999; Yuan, Quataert & Narayan 2003).

In this paper, we investigate the influence of outflow in more detail to check how good the above “standard treatment” is. We have derived the height-integrated accretion equations including the coupling between the inflow and outflow, to investigate the influence of outflow on the dynamics of inflow. We assume hydrostatic equilibrium for the inflow. For the outflow, we assume they are launched just above the surface of the inflow. We parameterize and estimate the quantities of outflow in terms of the quantities of inflow mainly from the results of numerical simulations. In this way, we reduce the numbers of unknown quantities in the above inflow/outflow equations thus we are able to get their global solution.

We have studied the influences on the dynamics of inflow of the strength (via vertical velocity), the (ion and electron) temperature, specific angular momentum, and the radial velocity of the outflow. We find that among them the strength of the outflow is the most important quantity. It can produce orders of magnitude difference for the density of inflow. If the strength of outflow is fixed, all other quantities of outflow can only produce a difference for the density and temperature within a factor of \sim two, if our estimations to the properties of outflow are correct. Therefore, the “standard treatment” is usually a good approximation.

The largest uncertainty in our model comes from the estimations to the properties of

outflow such as their temperature, specific angular momentum, azimuthal and radial velocity. We estimate these values from numerical simulations to accretion flows which is still not exact. With the rapid development of numerical simulation, our results will be significantly improved. Especially, if the properties of outflow is found to be far more deviated from the inflow than those adopted in the present paper (e.g., $\xi_{T_e} \gg 1$), the standard treatment will be not enough although we believe that our conclusion that the strength of outflow is the most influential quantity should remain correct. In that case, the influence of the other properties of outflow must be taken into account as well.

We thank our referee, Chris Done, for constructive suggestions. This work was supported in part by the Natural Science Foundation of China (grant 10773024), One-Hundred-Talent Program of China, and Shanghai Pujiang Program.

A. The height-integrated equations describing inflow/outflow

For a steady axisymmetric accretion flow, the equation of mass conservation is:

$$\frac{1}{r} \frac{\partial}{\partial r}(r\rho v_r) + \frac{\partial}{\partial z}(\rho v_z) = 0. \quad (\text{A1})$$

Defining the mass accretion rate $\dot{M} \equiv -4\pi r\rho v_r H$, we integrate eq. (A1) in z from 0 to H^+ , here H^+ denotes just above the surface $z = H$ where the outflow is just launched. Noting $v_z = 0$ for inflow and $v_z = v_{z,w}$ for outflow at H^+ , we get:

$$\frac{d\dot{M}}{dr} = \eta_1 4\pi r\rho v_{z,w}, \quad (\text{A2})$$

where

$$\eta_1 = \frac{\rho_w}{\bar{\rho}} = \frac{e^{-1/2}\rho(r, 0)}{\frac{1}{H} \int_0^H \rho(r, 0) \exp(-\frac{z^2}{2H^2}) dz} = 0.7089, \quad (\text{A3})$$

which gives the ratio of the density of outflow and height-averaged inflow.

The radial and azimuthal momentum equations read as follows:

$$\rho(v_r \frac{\partial v_r}{\partial r} - \frac{v_\phi^2}{r} + v_z \frac{\partial v_r}{\partial z}) = -\frac{\partial P}{\partial r} + \rho g_r, \quad (\text{A4})$$

$$\rho(v_r \frac{\partial v_\phi}{\partial r} + \frac{v_r v_\phi}{r} + v_z \frac{\partial v_\phi}{\partial z}) = \frac{1}{r^2} \frac{\partial}{\partial r}(r^2 \tau_{\phi r}). \quad (\text{A5})$$

Here g_r is the radial component of the gravitational force. The energy equation is

$$\rho T ds/dt \equiv \rho (dU/dt - P/\rho^2 d\rho/dt) = q^+ - q^-, \quad (\text{A6})$$

which for steady flow reduces to:

$$\rho \left[v_r \left(\frac{\partial U}{\partial r} - \frac{P}{\rho^2} \frac{\partial \rho}{\partial r} \right) + v_z \left(\frac{\partial U}{\partial z} - \frac{P}{\rho^2} \frac{\partial \rho}{\partial z} \right) \right] = q^+ - q^-. \quad (\text{A7})$$

We integrate the above equations A4-A7 for z from $z = 0$ to $z = H^+$ using the following general result:

$$\int_0^{H^+} f v_z \frac{\partial g}{\partial z} dz = f v_{z,w} (g_w - g_{z=H}), \quad (\text{A8})$$

where f and g are functions of (r, z) . Note that if $g(r, z)$ is continuous at $z = H$ (e.g., density ρ), the right side of equation (A8) is equal to 0. Then we will get eqs. (2) - (5).

REFERENCES

- Beckwith, K., Hawley, J. F., Krolik, J. H. 2008, astro-ph/0709.3833
- Blandford, R. D., Begelman, M. C. 1999, MNRAS, 303, L1 (BB99)
- Blandford, R. D., Begelman, M. C. 2004, MNRAS, 349, 68
- Blandford, R. D., Payne, D. G. 1982, MNRAS, 199, 883
- Chartas, G., Brandt, W. N., Gallagher, S. C. 2003, ApJ, 595, 85
- De Villiers, J.-P., Hawley, J. F., Krolik, J. H., Hirose, S. 2005, ApJ, 620, 878
- Granato, G. L., De Zotti, G., Silva, L., Bressan, A., Danese, L. 2004, ApJ, 600, 580
- Igumenshchev, I. G., Narayan, R., Abramowicz, M. A. 2003, ApJ, 592, 1042
- Kaspi, S., Brandt, W. N., George, I. M., et al. 2001, ApJ, 554, 216
- Kuncic, Z. & Bicknell, G. V. 2007, Ap&SS, 311, 127
- Gu, W., Lu, J. 2007, ApJ, 660, 541
- Marrone, D. P., Moran, J. M., Zhao, J. H., Rao, R. 2006, ApJ, 640, 308
- McKinney, J. C. 2006, MNRAS, 368, 1561
- Misra, R., & Taam, R. E. 2001, ApJ, 553, 978
- Narayan, R., Yi, I. 1994, ApJ, 428, L13

- Narayan, R., Yi, I. 1995, ApJ, 444, 231
- Paczynski, B., Wiita, P. J. 1980, A&A, 88, 23
- Proga, D. 2003, ApJ, 585, 406
- Quataert, E., Narayan, R. 1999, ApJ, 520, 298
- Silk, J., Rees, M. J. 1998, A&A, 331, L1
- Shakura, N. I., Syunyaev, R. A. 1973, A&A, 24, 337
- Springel, V., Di Matteo, T., Hernquist, L. 2005, MNRAS, 361, 776
- Spruit, H. C. 1996, in Physical processes in Binary Stars, eds. R.A.M.J. Wijers, M.B. Davies and C.A. Tout, (NATO ASI Series, Kluwer Dordrecht), astro-ph/9602022
- Stone, J. M., Pringle, J. E. 2001, MNRAS, 322, 461
- Stone, J. M., Pringle, J. E., Begelman, M. C. 1999, MNRAS, 310, 1002
- Xu, G., Chen, X. 1997, ApJ, 489, L29
- Xue, L., Wang, J. 2005, ApJ, 623, 372
- Yuan, F., Quataert, E., Narayan, R. 2003, ApJ, 598, 301
- Vlahakis, N., Königl, A. 2003, ApJ, 596, 1080

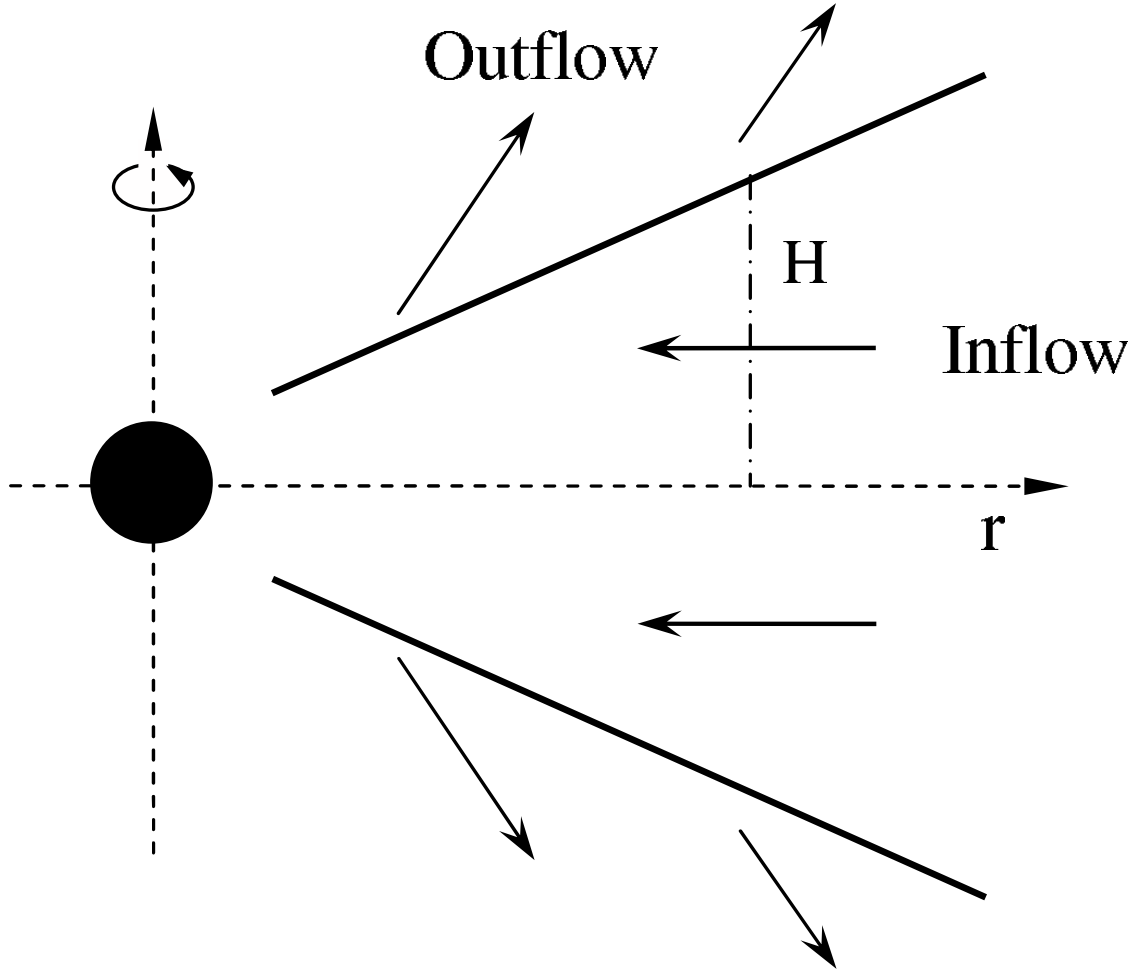


Fig. 1.— Schematic diagram of inflow/outflow model. Outflow launches from the surface $z = H$.

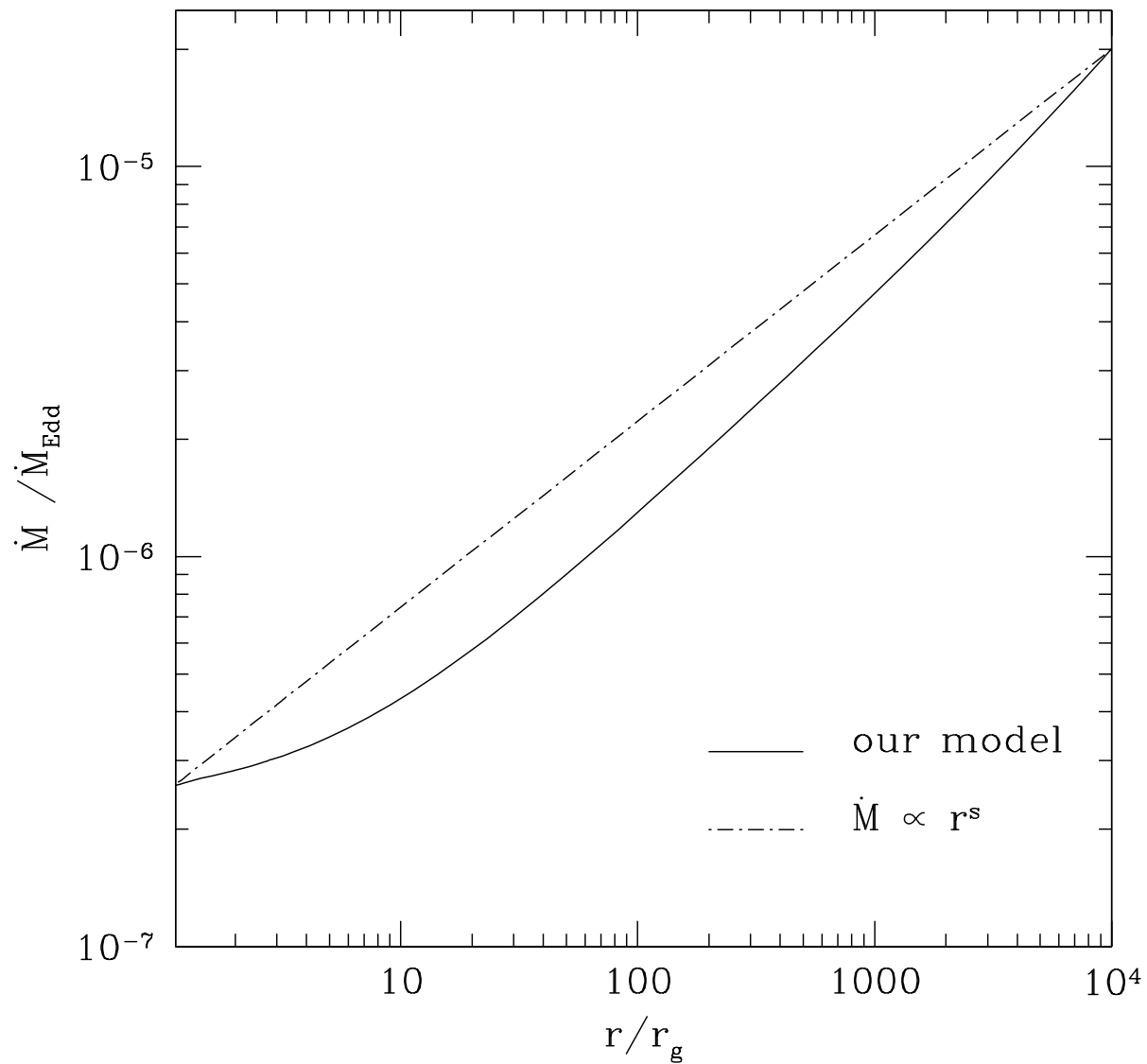


Fig. 2.— The change of accretion rate as a function of radius for our model (solid line) and the standard treatment (dashed line) in which $\dot{M}(r) \propto r^s$ with s being a constant.

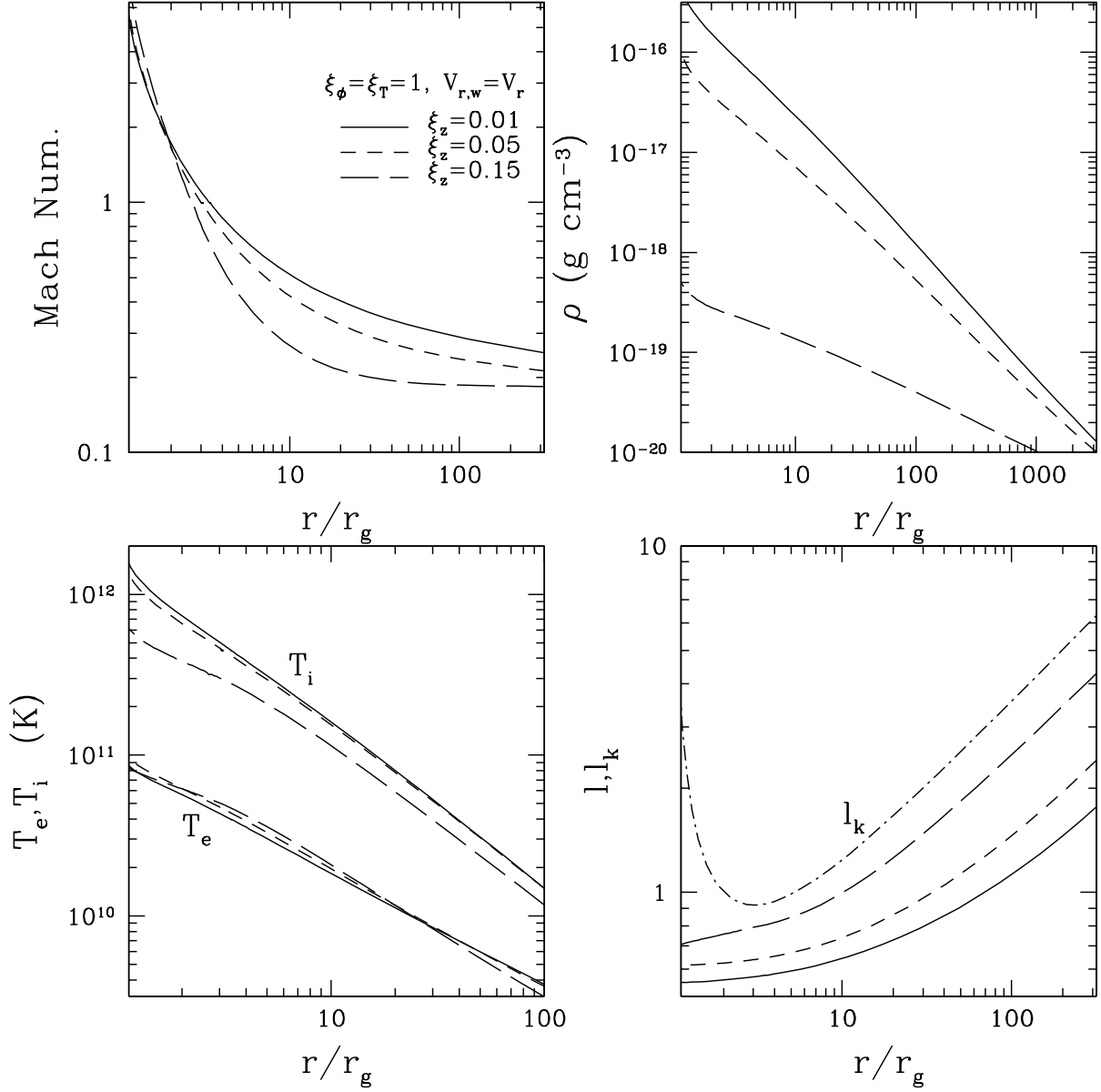


Fig. 3.— Influence of the vertical velocity of the outflow described by ξ_z on the Mach number, density, temperature, and specific angular momentum of inflow. The solid, dashed, and long-dashed lines are for $\xi_z = 0.01, 0.05, 0.15$, respectively. The Keplerian angular momentum l_k is shown as the dot-dashed line in the bottom right panel. Other parameters are $v_{r,w} = v_r$, $\xi_\phi = \xi_{T_e} = \xi_{T_i} = 1.0$.

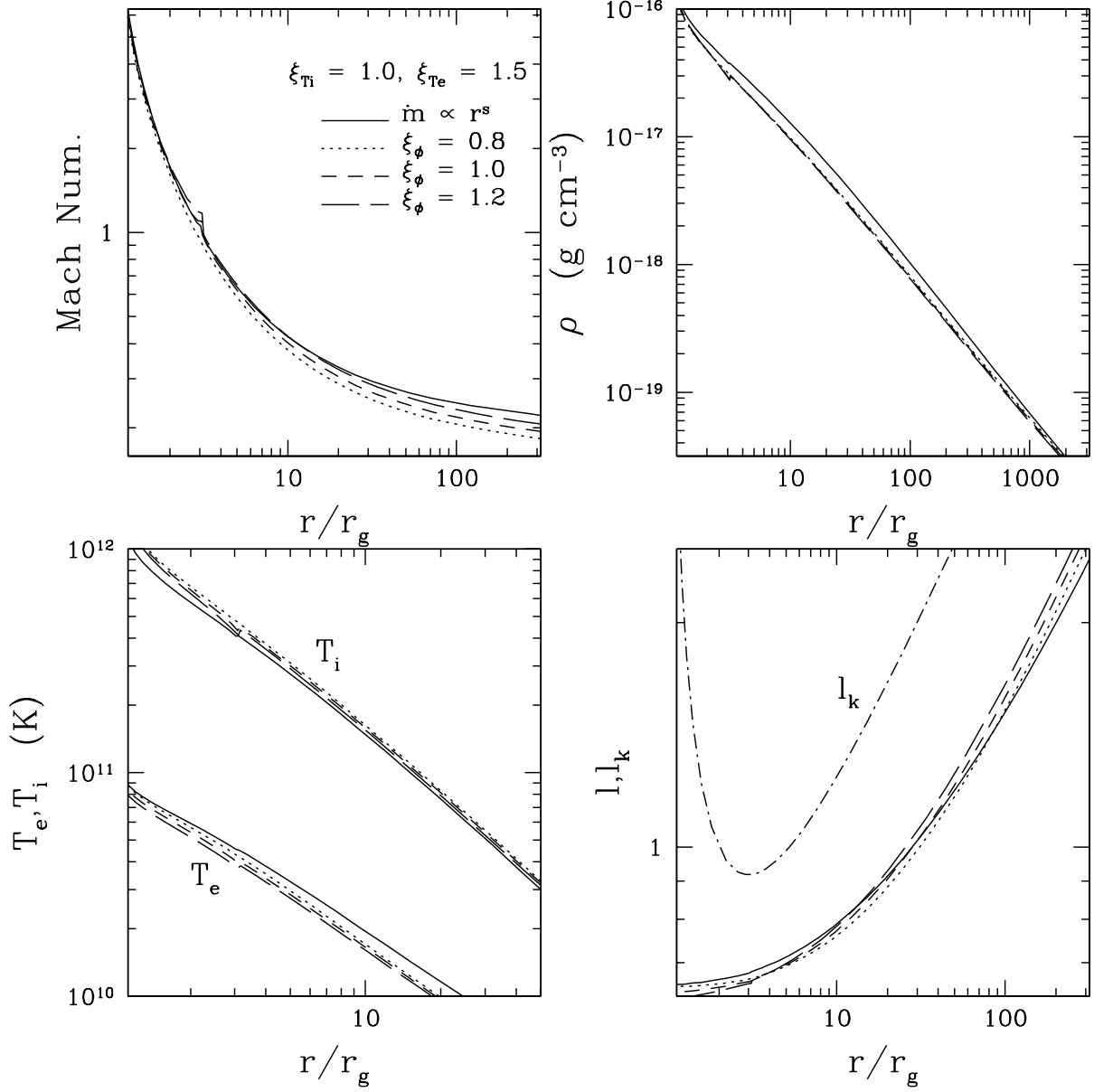


Fig. 4.— Influence of the specific angular momentum of the outflow described by ξ_ϕ on the dynamics of inflow and their comparison with the standard treatment (solid line). The dotted, dashed, and long-dashed lines are for $\xi_\phi = 0.8, 1.0, 1.2$, respectively. Other parameters are $\xi_{Ti} = 1$ (Case A), $\xi_r = 0.2$, $\xi_{Te} = 1.5$. We adjust ξ_z so that all the four models have the same accretion rates at the inner and outer boundary.

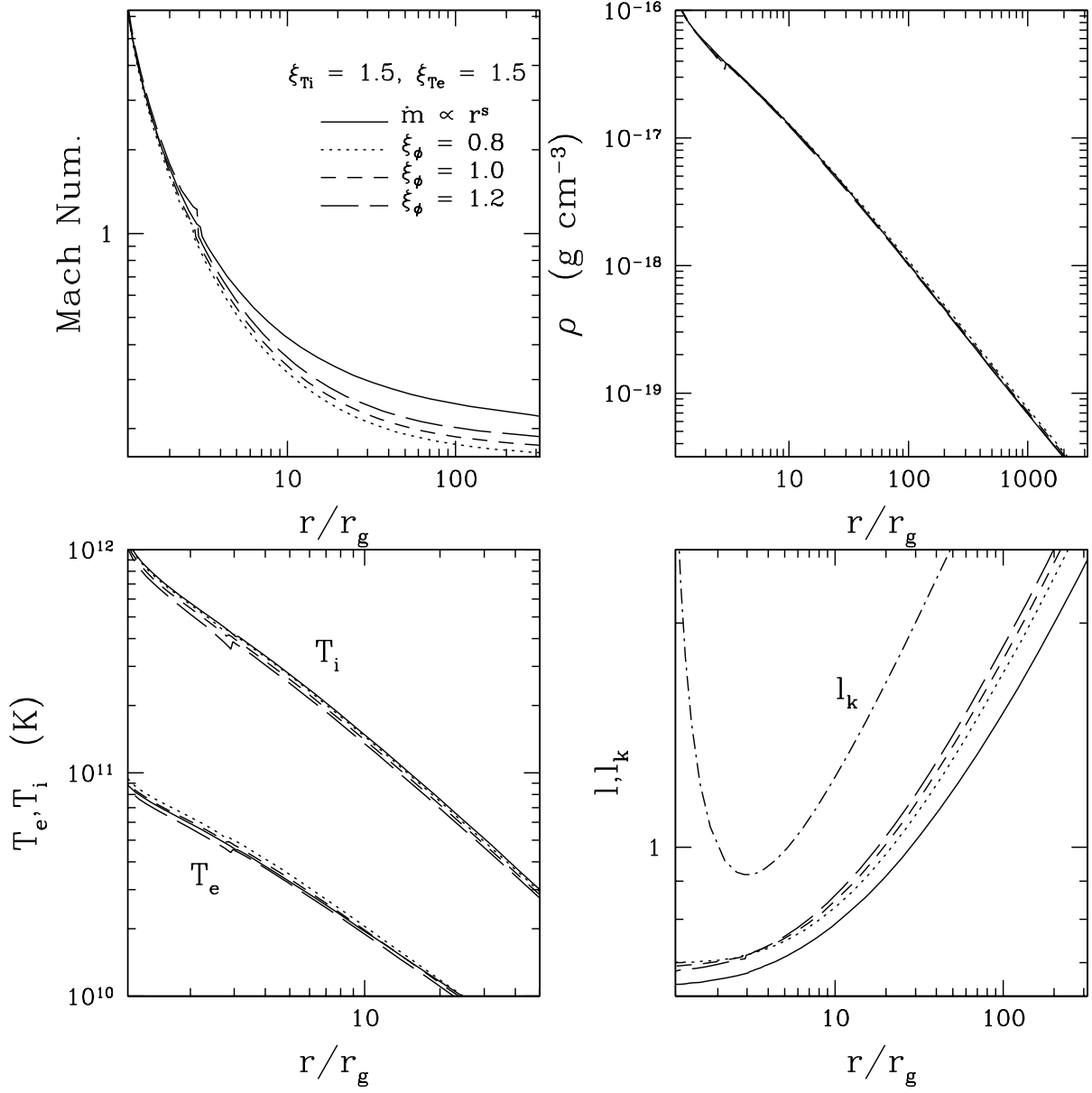


Fig. 5.— Influence of the specific angular momentum of the outflow on the dynamics of inflow and their comparison with the standard treatment. All parameters are the same as Fig. 4 (Case A) except $\xi_{Ti} = 1.5$.